Effective Interface Hamiltonians for Unbinding Transitions in Ternary Amphiphilic Mixtures

F. Clarysse[1] **and C. J. Boulter**[2,*]

[1] Laboratorium voor Vaste-Stoffysica en Magnetisme, Katholieke Universiteit Leuven, Celestijnenlaan 200D, B-3001 Leuven, Belgium.

[2] Department of Mathematics, Heriot-Watt University, Edinburgh EH14 4AS, United Kingdom.

[*] To whom correspondence should be addressed.

Abstract

We outline an analytic method for deriving effective interfacial models, suitable for describing unbinding behaviour in ternary amphiphilic mixtures, from underlying non-critical bulk models. Herein we concentrate on deriving interfacial properties (the surface tension and rigidity coefficients) for the simple case of a free oil-phase/microemulsion interface. This calculation allows us to explicitly demonstrate the difference between the interfacial tension, which is a uniquely defined quantity, and the rigidities which are highly sensitive to the choice of interface location definition.

We conclude by describing how the model derivation may be extended to include the effect of an external surface, which is appropriate for the study of wetting in a confined ternary mixture. We briefly summarize the results of a recent study of wetting at such a surface for which a rich phase diagram is predicted.

Keywords : Wetting transitions, ternary mixtures, interfacial tension, method of calculation

INTRODUCTION

In this paper we present an overview of our recently introduced method for deriving an effective interface Hamiltonian suitable for ternary mixtures [1,2], the ubiquitous example being a mixture of oil, water and surfactant or amphiphile. These mixtures have recently attracted much attention partly due to the wide range of different phases which may be observed. These include micellar solutions, the lamellar phase (a stack of monolayers separated by oil-rich or water-rich regions), and a microemulsion or middle-phase characterized by a random array of monolayers (for a detailed review see [3]).

Our goal here is to provide a tutorial summary of our approach. In order to afford a clear exposition we consider a new example of a free oil-phase/microemulsion interface, and explicitly derive the interfacial tension and rigidity coefficients appearing in the model. While some of these results can be obtained by other techniques, this choice does allow a useful demonstration of the method of calculation incorporating all the key features in a simple example. In the final section we briefly discuss extending the approach to incorporate external surfaces and review results found for wetting of such surfaces in ternary mixtures.

INTERFACE MODEL DERIVATION

Our goal in this section is to derive an effective interface model for a free interface between two coexisting phases. We identify three homogeneous phases $+$, $-$ and middle (which can be associated with the oil, water and microemulsion respectively) with symmetry between the $+$ and $-$ phases. We base our analysis on a simple Ginzburg-Landau free-energy functional

$$\mathcal{H}[\phi] = \int \mathrm{d}\mathbf{r} \left\{ c(\nabla^2\phi)^2 + g(\phi)(\nabla\phi)^2 + f(\phi) - \mu\phi \right\}, \tag{1}$$

where $\phi(\mathbf{r})$ is the order-parameter representing the local concentration difference between + and − phases. Here we fix the chemical potential difference between oil and water, μ, to zero, while the bulk free-energy density, $f(\phi)$, has three coexisting minima corresponding to the three homogeneous phases. From comparison with scattering experiments we know $g(\phi)$ is negative in the middle (microemulsion) phase but is positive in the pure + and −-phases. Finally c is always positive, stabilizing the system, and for simplicity may be assumed constant.

In order to derive an interface Hamiltonian from this model we follow the approach of Fisher and Jin [4] and introduce a crossing constraint definition of the collective coordinate l. This involves finding the density profile $\phi(\mathbf{y}, z)$ which satisfies the constraint $\phi(\mathbf{y}, z = l(\mathbf{y})) = \phi^X$ where ϕ^X is a reference crossing value. Here z is the coordinate direction perpendicular to the interface while $\mathbf{y}$ represents the $d-1$ coordinates in the plane of the interface. We denote the constrained profile by $\phi_\Xi(\mathbf{y}, z; l(\mathbf{y}))$. In what follows we consider situations in which the order-parameter profile is oscillatory and so to ensure that the interface location is uniquely defined we demand that l is the location where the profile *first* crosses the reference value. The key observation of [4] is that it is most convenient to expand about the *planar* constrained profile, $\phi_\pi(z; z^X)$ say, which satisfies $\phi_\pi(z = z^X) = \phi^X \ \ \forall \mathbf{y}$ with z^X some arbitrary reference plane.. Following this approach we derive an expansion for ϕ_Ξ of the form

$$\phi_\Xi(\mathbf{y}, z; l(\mathbf{y})) = \phi_\pi(z; l(\mathbf{y})) + B_1(z; z^X)(\nabla^2 l) + B_2(z; z^X)(\nabla l)^2 + \ldots \qquad (2)$$

Here the ellipsis represents higher order gradient terms which do not play a role in our analysis and the functions ϕ_π, B_1 and B_2 satisfy simple differential equations [2]. We note that for a free interface the leading order term in the expansion $\phi_\pi(z; l(\mathbf{y})) \equiv \phi_\pi(z - l(\mathbf{y}))$ and simply corresponds to a rigid shift of the equilib-

rium free interface. Formally we identify the interface Hamiltonian, $\mathcal{H}_I[l]$, via a partial trace taken over those states which are compatible with the given interface configuration. In practice we accept the simpler saddle-point identification

$$\mathcal{H}_I[l(\mathbf{y})] \equiv \mathcal{H}[\phi_\Xi(\mathbf{r}; l(\mathbf{y}))] \tag{3}$$

so ϕ_Ξ is just the interfacial profile which minimizes $\mathcal{H}[\phi]$ subject to the constraint represented by the interface configuration $l(\mathbf{y})$. With this definition we derive an effective interface model

$$\mathcal{H}_I[l] = \int \mathrm{d}\mathbf{y} \left\{ \frac{1}{2}\Sigma_{\mathrm{free}}(\nabla l)^2 + \frac{1}{2}\kappa_{\mathrm{free}}(\nabla^2 l)^2 + \frac{1}{2}\rho_{\mathrm{free}}(\nabla l)^4 \right\} \tag{4}$$

where Σ_{free} is the interfacial stiffness, and κ_{free} and ρ_{free} are rigidity coefficients. These coefficients may be explicitly identified as follows

$$\Sigma_{\mathrm{free}} = \int_{-\infty}^{\infty} \mathrm{d}z \left\{ 4c \left(\frac{\partial^2 \phi_\pi}{\partial z^2} \right)^2 + 2g(\phi_\pi) \left(\frac{\partial \phi_\pi}{\partial z} \right)^2 \right\}, \tag{5}$$

$$\kappa_{\mathrm{free}} = \int_{-\infty}^{\infty} \mathrm{d}z \left\{ 2c \left(\frac{\partial \phi_\pi}{\partial z} \right)^2 + 2g(\phi_\pi) \frac{\partial \phi_\pi}{\partial z} B_1 - 4c \frac{\partial^3 \phi_\pi}{\partial z^3} B_1 \right\}, \tag{6}$$

and

$$\rho_{\mathrm{free}} = \int_{-\infty}^{\infty} \mathrm{d}z \left\{ 2c \left(\frac{\partial^2 \phi_\pi}{\partial z^2} \right)^2 + 3g'(\phi_\pi) \left(\frac{\partial \phi_\pi}{\partial z} \right)^2 B_2 + 2g(\phi_\pi) \frac{\partial^2 \phi_\pi}{\partial z^2} B_2 \right\}. \tag{7}$$

As mentioned above the planar profiles, ϕ_π, for different choices of crossing value ϕ^X are simply related by a rigid shift and hence the value of Σ_{free} given by (5) is independent of ϕ^X – i.e. the surface tension of the free interface is uniquely defined.

In contrast the functions B_1 and B_2 depend strongly on the choice of crossing value with, for example, both functions vanishing when $z = z^X$ such that different choices of ϕ^X will result in different locations of the zeroes of these functions. As a

consequence the values of both κ_{free} and ρ_{free} are specific to the choice of crossing value (we shall demonstrate this with a concrete example in the next section).

We note that these results are consistent with earlier analyses of free interfaces by other authors [5–7] with in particular the Gaussian coefficients Σ_{free} and κ_{free} being obtainable from a variety of different routes. However the method we have outlined here allows the inclusion of terms beyond Gaussian level, and more importantly can be extended to include external surfaces or walls without significant complication – we shall return to this issue in more detail in the final section.

FREE OIL/MICROEMULSION INTERFACE

In this section we will apply the formalism given above to the specific example of a +-phase/middle phase interface. This will demonstrate the main results concerning the dependence of the gradient coefficients upon ϕ^X while highlighting the key mathematical problems faced when applying the method to more difficult examples.

To begin we introduce a triple parabola model (TPM) to approximate the free energy densities in the Ginzburg-Landau model (1). In this model the bulk density $f(\phi)$ is approximated by a number of parabolas whereas $g(\phi)$ is modelled by a piecewise constant function (see [3] for more details). We assume the system displays three-phase coexistence of a +-phase with $\phi = \phi_+ > 0$, a $-$-phase with $\phi = \phi_- < 0$ and a middle phase with $\phi = \phi_m = 0$. The TPM form for $f(\phi)$ is

$$f(\phi) = \begin{cases} \omega_+(\phi - \phi_+)^2, & \phi > \phi_{0,+} \\ \omega_m\phi^2 + f_0, & \phi_{0,-} < \phi < \phi_{0,+} \\ \omega_-(\phi - \phi_-)^2, & \phi < \phi_{0,-} \end{cases} \tag{8}$$

where $\phi_{0,+}$ and $\phi_{0,-}$ are chosen such that f is continuous. The demand of three-

phase coexistence further implies that the three local minima must be of equal depth and so f_0 has to be taken zero. We must also set the chemical potential difference μ between oil and water in (1) to zero as noted earlier. Finally, $g(\phi)$ is given in this model by

$$g(\phi) = \begin{cases} g_+, & \phi > \phi_{0,+} \\ g_m, & \phi_{0,-} < \phi < \phi_{0,+} \\ g_-, & \phi < \phi_{0,-} \end{cases} \tag{9}$$

Appropriate values for the constants may be elucidated from scattering experiments in the three homogeneous phases, these clearly show that both in the oil and water phases the function $g(\phi)$ must be strictly positive. Thus, $g_+ > 0$ and $g_- > 0$. However, in the microemulsion phase a pronounced peak in the scattering intensity at nonzero wavevector q is found when a strong amphiphile is used demonstrating that g_m is negative in that case.

For convenience we focus here on systems with oil-water symmetry, and choose $\phi_+ = -\phi_- = 1$, $\omega_+ = \omega_- = 4$, $\omega_m = 1$, $c = 1$, and $g_+ = g_- = 4.5$. For this choice the bulk phase diagram is well known and exhibits three regions. The first region supports coexisting oil-rich and water-rich phases (i.e. + and −-phases), in the second the microemulsion or middle-phase is stable while in the third it is the lamellar phase which is found. For our study we wish to sit at three phase coexistence between +, − and middle-phases which means we need to sit on the phase boundary given by $f_0 = 0$ and $g_m > -2$ [3]. We make the specific choice $g_m = -1$ which corresponds to a region where the correlation function in the middle phase displays an oscillatory behaviour, as does the free +-phase/middle phase interface.

The choice of a piecewise parabolic model is motivated by the observation

that the equations governing the planar profile and the B_i functions can be solved analytically in this case and essentially yield sums of exponential functions. In addition, previous studies suggest that the use of completely smooth functions for f and g would give the same qualitative results but require the introduction of more complicated numerical techniques [8]. However, a negative feature of this model is that for a general choice of crossing value ϕ^X one finds that the 'interface width' is a free parameter in the TPM which must be determined by further minimization. In particular for the choice of parameters described above we find $\phi_{0,+} = 2/3$, for simplicity assume $\phi_\pi(z = 0) = 2/3$ along with the crossing condition $\phi_\pi(z^X) = \phi^X$. Hence if we choose $0 \leq \phi^X < 2/3$ say, then we must solve the Euler-Lagrange equation arising from minimising $\mathcal{H}[\phi]$ in each of the three regions : $z > z^X$, $0 < z < z^X$, and $z < 0$, and in addition impose the asymptotic conditions $\phi(z \to \infty) = 0$ and $\phi(z \to -\infty) = 1$ plus conditions of continuity and smoothness. We can associate z^X with the interface width and we find that solutions are possible for many choices of this parameter with the optimal constrained profile being given by the choice of z^X which minimizes the free energy.

An example of such a profile is given in Fig. 1 for the choice $\phi^X = 0$. In this case the optimal interface width is found to be $z^X \approx 1.8$. We note that for this example the oscillations in the profile are small and occur over a limited range, however if we decrease the value of g_m towards -2 the size and number of oscillations increases consistent with the fact we are approaching the region of the phase diagram where the lamellar phase is the stable one. In Fig. 2 we show the corresponding results for the functions $B_1(z)$ (solid line) and $B_2(z)$ (dashed line) appearing in the gradient expansion (2). Note that these functions must vanish

at both $z = 0$ and $z = z^X$, so that their form is qualitatively different for different choices of ϕ^X in contrast to the constrained planar profile. As we discussed in the last section this results in a ϕ^X dependence for the rigidity coefficients $\kappa_{\rm free}$ and $\rho_{\rm free}$ not found in the stiffness $\Sigma_{\rm free}$. This is clearly demonstrated in Fig. 3 where we plot the stiffness and rigidity coefficients as a function of ϕ^X. Our final observation in this section is that our result for $\kappa_{\rm free}(\phi^X)$ is consistent with the known inequality $\kappa_{\rm free}(\phi^X) \leq \kappa_{\rm rs}$ [6] where $\kappa_{\rm rs}$ is the rigid-shift contribution to $\kappa_{\rm free}$ (i.e. the result one would find upon setting B_1 and B_2 identically to zero) which for our model is $\kappa_{\rm rs} \approx 0.600$.

WETTING OF AN EXTERNAL SURFACE

In this section we describe the extension of our analysis to the situation where an external wall is included. Full details of this calculation can be found in [2] so here we only highlight the key differences to the analysis of the last section and provide a summary of the main results. We consider a semi-infinite geometry with a surface in the plane $z = 0$, and now use $\mathbf{y}$ to denote the $d-1$ dimensional vector displacement along this surface. We assume that the +-phase is preferred at the surface and that the middle phase is stable in the bulk, and denote the interface between the two phases (where $\phi \equiv \phi^X$) by $l(\mathbf{y})$. To model this situation we must include an additional surface density term $\int {\rm d}\mathbf{r}\delta(z)\left\{\mu_s\phi + \omega_s\phi^2 + g_s(\nabla\phi)^2\right\}$ in our Ginzburg-Landau free energy functional (1). This expression is characterized by three surface parameters. The chemical potential (μ_s), the surface enhancement (ω_s) and a gradient parameter (g_s) which can be associated with the local chemical potential of the amphiphile at the wall [9].

We again make a gradient expansion for the constrained interfacial profile and derive an interface model similar to (4). However in this case the gradient coef-

ficients include a weak position-dependence and we must include the additional term $\int \mathrm{d}\mathbf{y} W(l)$ where $W(l)$ is the interface potential describing the interaction of the fluctuating interface with the external surface. For the scenario we are considering here this interface or binding potential is given explicitly by

$$\begin{aligned} W(l) &= \int_0^\infty \mathrm{d}z \left\{ c\left(\frac{\partial^2\phi_\pi}{\partial z^2}\right)^2 + g(\phi_\pi)\left(\frac{\partial\phi_\pi}{\partial z}\right)^2 + f(\phi_\pi)\right\} \\ &\quad + \left[\mu_s\phi_\pi + \omega_s\phi_\pi^2 + g_s\left(\frac{\partial\phi_\pi}{\partial z}\right)^2\right]_{z=0}, \end{aligned} \tag{10}$$

ignoring l-independent terms. At the mean-field level the binding potential is all we require to analyse possible wetting of the wall-middle phase interface by the +-phase. In particular the interface location is given by the minimum of $W(l)$, so a wetting transition is predicted whenever the location of the minimum diverges. By determining the interface potential as a function of the surface parameters one can derive a complete surface phase diagram for the system.

Using this method we predict a rich phase diagram containing both first-order and continuous wetting transitions. For example, when $g_s = 1$ and $\mu_s = -2$ we find a first order wetting transition as we reduce ω_s from a large positive value; for $\omega_s > 0.527$ the interface potential has its global minimum at $l \approx 1.8$ while for $\omega_s < 0.527$ the global minimum is at infinity but a local minimum remains at $l \approx 1.8$ until $\omega_s = -0.161$. This point may be identified as a metastable limit beyond which the only minimum of the potential is at infinity. A similar limit exists at $\omega_s = 1$ when the extremum at infinity changes nature from a minimum to a maximum.

For some choices of surface parameters we observe very different behaviour where the location of the global minimum of $W(l)$ diverges continuously as we approach the transition boundary, corresponding to a continuous wetting tran-

sition. In general, for a given choice of surface parameter g_s we find first-order transitions for smaller values of $|\mu_s|$ and continuous transitions for larger $|\mu_s|$. Recall we only consider negative μ_s values here as appropriate for wetting by the +-phase, however due to the symmetry of our system we predict analogous behaviour for positive μ_s with the −-phase wetting the wall-middle phase interface. The surface phase diagram for the case $g_s = 1$ is given in Fig. 4, showing first order (FW) and continuous wetting transition phase boundaries. The two lines meet at a tricritical point (TCP) which is also the terminus for the two metastable limits (dashed lines) discussed above. In the vicinity of the TCP we further find a (first-order) thin-thick transition which may precede the wetting transition (see inset of Fig. 4). The corresponding thin-thick transition line extends from a triple point on the FW line and terminates at a surface critical point where the layer thicknesses on each side of the transition become the same. We stress that the thin-thick transition is not an artefact of the crossing criterion definition of l but can be understood in terms of oscillations in the binding potential. These are on the scale of 10^{-5} and hence are typically overlooked, however close to TCP both the depth of the minimum at finite l and the height of the potential barrier are of this order and the oscillations become important. In principle further layering transitions may also be expected although we have been unable to locate such transitions due to the very small energy differences involved.

We note that the choice $g_s = 1$ used above is completely arbitrary and that our results are robust to variations in this parameter. That is, for other values of g_s (including $g_s \leq 0$) we obtain a qualitatively identical picture. The main quantitative difference is that we find a larger region of the first-order wetting transition when we use smaller, or negative, values of g_s (i.e. the FW transition

line extends over a wider range of μ_s values than shown in Fig. 4). Hence we find transitions occurring for positive and negative values of all three surface parameters and consequently believe this wetting transition should be accessible in experimental systems. An appropriate experimental study is proposed in [1] for a system containing non-ionic amphiphiles. In such systems van der Waals forces must be included and lead to some modifications of the phase behaviour we have predicted above. The magnitude of the fluid-fluid forces is anticipated to be rather small because the densities of all three phases are very close to one another. Hence we only consider the inclusion of a long-range substrate potential which effectively adds a term of the form a/l^2 to the interface potential. The Hamaker constant, a, is proportional to the difference in densities of the wetting phase and the bulk phase. Hence if we assume the adsorbed phase is the oil-rich one then $a < 0$ and the unbinding transition is suppressed. However if the adsorbed phase is the water-rich one then $a > 0$ and the unbinding transition remains although only first-order transitions will now be observed. Consequently we predict first-order wetting transitions should be experimentally observable provided the substrate is treated such that the (denser) water-rich phase is preferred (see for example [10]).

CONCLUSIONS

In this paper we have introduced a technique for accurately deriving an effective Hamiltonian suitable for studying interface and unbinding behaviour in ternary amphiphilic mixtures. Such an approach is appropriate for studying free interfacial properties, interactions between fluctuating interfaces (such as in the lamellar phase), and to study unbinding and adsorption effects where external surfaces are present. Herein we have primarily concentrated on studying a free +-phase/middle phase interface and have calculated the stiffness and rigidity co-

efficients. Within a piecewise parabolic model we have explicitly demonstrated that the surface tension is a uniquely defined property whereas the rigidities are specific to the choice of interface location definition.

Finally we have applied our model to study the possibility of wetting of a wall/middle phase interface by the +-phase, as might be appropriate in the analysis of confined microemulsions. We predict a rich mean-field surface phase diagram containing thin-thick transitions and both continuous and first-order wetting transitions. Future work will concentrate on determining the effect of the stiffness and rigidity coefficients on critical behaviour when we extend our study beyond mean-field level.

ACKNOWLEDGMENTS

This research has been supported by the Project VIS/97/01 of the Flemish Government, the Inter-University Attraction Poles (IUAP), the Concerted Action Research Programme (GOA), and the Nuffield Foundation (NUF-NAL 99).

REFERENCES

[1] C.J. Boulter and F. Clarysse, Phys. Rev. E, 60 (1999) R2472–R2475.

[2] F. Clarysse and C.J. Boulter, Physica A, 278 (2000) 356–389.

[3] G. Gompper and M. Schick, Self-Assembling Amphiphilic Systems (Vol. 16 Phase Transitions and Critical Phenomena), Academic Press, London, 1995.

[4] M.E. Fisher and A.J. Jin, Phys. Rev. Lett., 69 (1992) 792–795.

[5] G. Gompper and M. Kraus, Phys. Rev. E, 47 (1993) 4289–4300.

[6] A.O. Parry and C.J. Boulter, J. Phys.:Condens. Matter, 6 (1994) 7199–7206.

[7] A. Robledo and C. Varea, J. Stat. Phys., 89 (1997) 273–282.

[8] G. Gompper and M. Hennes, J. Chem. Phys., 102 (1995) 2871–2880.

[9] G. Gompper and S. Zschocke, Phys. Rev. A, 46 (1992) 4836–4851.

[10] X.-L. Wu, M. Schlossman and C. Franck, Phys. Rev. B, 33 (1986) 402–412.

FIGURE CAPTIONS

Figure 1 : Planar profile of the free +-phase/middle-phase interface calculated in the symmetric triple parabola model with parameter values $c = 1$, $\omega_m = 1$, $\omega_+ = 4$, $g_m = -1$, $g_+ = 4.5$ and $\phi_+ = 1$. Here the reference value $\phi^X = 0$ has been used.

Figure 2 : Plot of the functions $B_1(z)$ (solid line) and $B_2(z)$ (dashed line) appearing in the expansion of the full constrained interface profile, calculated in the symmetric triple parabola model with parameter values as given in figure 1.

Figure 3 : The gradient coefficients Σ_{free}, κ_{free} and ρ_{free} for a range of crossing values ϕ^X. The parameters have been calculated within the triple parabola model with parameter values as given in figure 1.

Figure 4 : Mean-field surface phase diagram for the case $g_s = 1$, calculated within the symmetric piecewise parabolic model. First-order (FW) and continuous (CW) wetting phase boundaries are shown by solid lines; the two regimes are separated by a tricritical point (TCP). In the vicinity of TCP a thin-thick transition can occur (see inset). The thin-thick transition boundary begins at a triple point (TP) on the FW line and terminates at a surface critical point (SCP). The dashed lines denote metastable limits for the transitions.

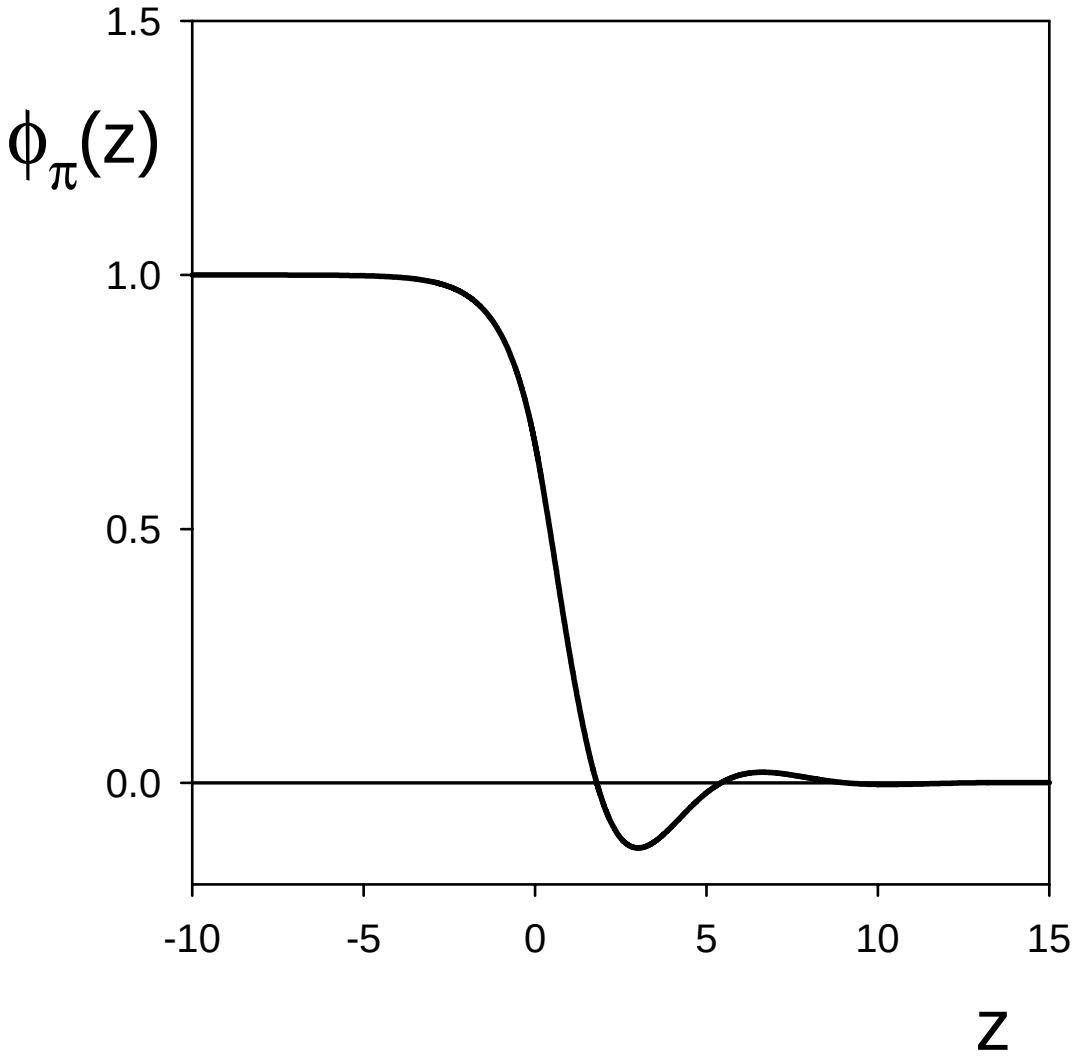

Figure 1: Clarysse and Boulter

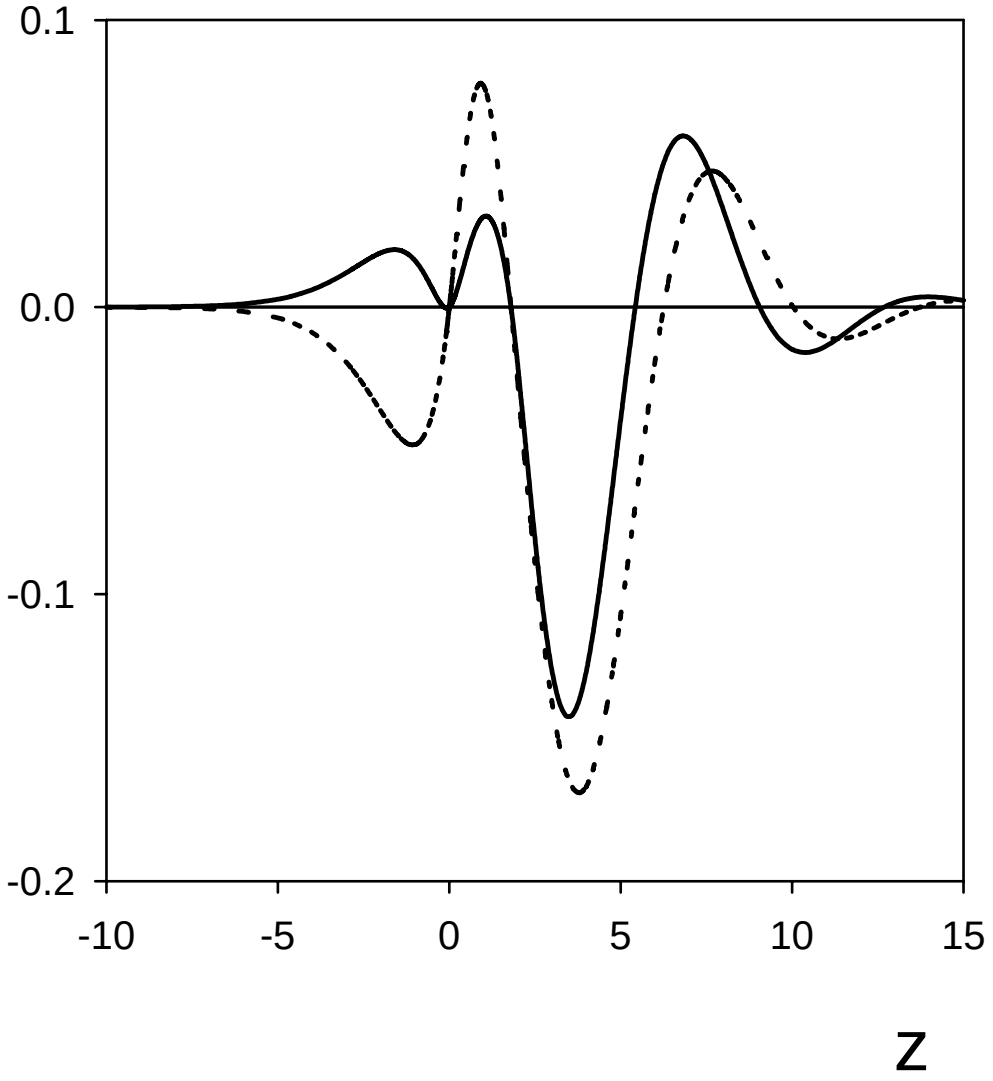

Figure 2: Clarysse and Boulter

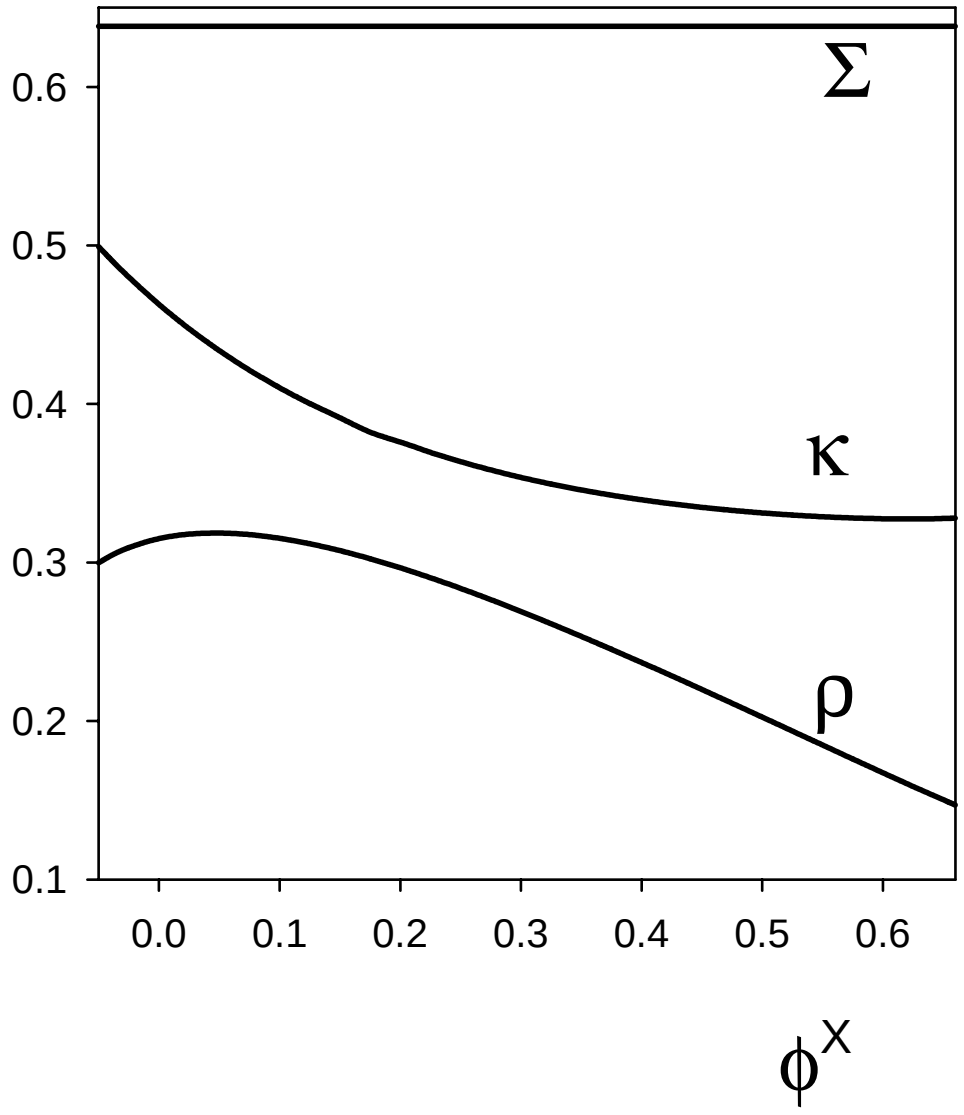

Figure 3: Clarysse and Boulter

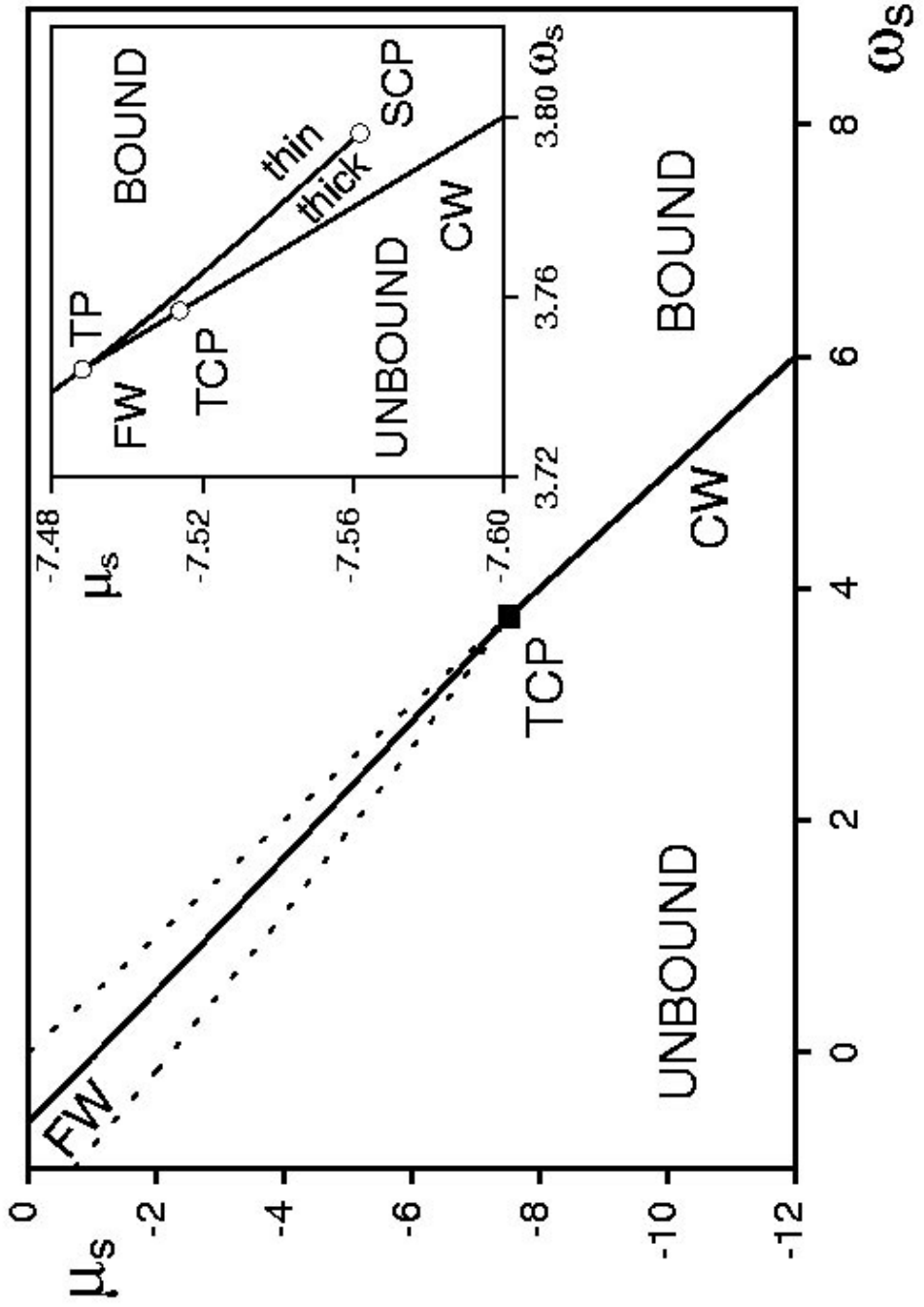

Figure 4: Clarysse and Boulter